

Development of Bottom Blowing Distribution Design on Top and Bottom Blowing Converter

B. J. LI*, C. C. HOU*, H. W. HSU*, T. K. YEH*,
P. T. CHENG*, C. W. YU* and Y. T. HUANG**

*Steelmaking Department

**Iron and Steel Research & Development Department
China Steel Corporation

In recent years, the international steel industry has faced severe overcapacity, leading to significant challenges for the domestic steel industry. In January 2020, CSC announced that the focus of development for the next fifty years would be on high-value refined steel plants. To meet the anticipated surge in demand for high-value refined steel, the converter factory actively pursued a bottom-blowing improvement to enhance the metallurgical effect. By collecting past metallurgy data, analyzing furnace lining erosion, and using innovative bottom-blowing flow simulation technology, the converters were finally optimized with a novel bottom-blowing distribution. CSC successfully developed high-efficiency, long-life top and bottom combined blowing technology of a 150-ton converter.

In the past, towards the end of lining life, excessive erosion of the bottom blowing tuyere bricks necessitated stopping the supply of bottom blowing gas. It deteriorated the steel-slag reaction kinetics and significantly reduced the metallurgical effect. Through the bottom blowing distribution modification, the full period of lining life with bottom blowing was successfully achieved. Total iron content in the slag is effectively reduced by 2% and thereby liquid steel output increases. In addition, the erosion rate of tuyere bricks decreases by at least 10% and then the furnace lining life can be increased by approximately 500 cycles by using the optimal design. Even towards the end of the lining life, high-quality ultra-low phosphorus steel still can be produced. It demonstrates that the improvement of bottom blowing not only improves the lining erosion but also keeps metallurgical performance throughout the entire lining life.

Keywords: BOF steelmaking, Bottom blowing distribution, Lining erosion, Bath mixing

1. INTRODUCTION

Due to the anticipated surge in demand for premium steel products with high value, it is much more important to develop efficient dephosphorization in converters and maintain the bottom blowing technology to the shut-down. Before the modification of the 150-ton converter in CSC, the gas supply for bottom blowing was gradually shut off according to the remaining thickness of each tuyere brick and finally, the converter had lost its bottom blowing capability. Poor bottom blowing affects the metallurgical performance and limits the product that can be produced. In addition, the lower the thickness of the tuyere brick, the higher the risk of steel leakage from the converter. This risk also impacts the production schedule. Collect research on bottom blowing, focusing mainly on blowing intensity, distribution, blowing gas, and bottom blowing elements⁽¹⁻³⁾. This study focuses on bottom blowing distribution.

The previous bottom blowing distribution of 150-

ton converters in CSC were respectively 4-hole concentric and 6-hole non-concentric. In 2021, during the shell and trunnion replacement of the converters, an attempt was made to modify the bottom tuyere distribution to a 6-hole concentric design. According to the literature, the optimal bottom tuyere distribution ranges between $0.40D$ and $0.65D^{(4)}$, where D is the diameter of the molten bath. We designed a new bottom blowing distribution, which extended the tuyere position closer to the wall shell. The concentric design makes the construction of the bottom lining much easier. The new tuyere positions, farther from the center, are expected to reduce dead zones and shorten homogenization time. However, the performance of the above-mentioned modification not only failed to meet expectations but also resulted in abnormal erosion of the furnace lining.

At the same time, a new 8-hole non-concentric bottom tuyere distribution was proposed. This design was based on the old 6-hole non-concentric and added two bottom tuyere positions near the charging side. Previous

experience shows that the farther the bottom tuyere position is to the tapping side, the shorter the soaked time in the interface between slag and steel during the period of tapping. We also compared past metallurgy data and furnace lining erosion data across all designs and used innovative simulation techniques for the bottom blowing flow field. A novel 8-hole bottom blowing distribution for the 150-ton converter was developed. This article presents the metallurgy data, furnace lining erosion rates, and mixed flow simulation for the four cases.

2. EXPERIMENTAL

At CSC, four types of bottom blowing distributions were used: 4-hole concentric, 6-hole non-concentric, 6-hole concentric, and 8-hole non-concentric. We simulated the bath mixing behavior for each distribution as shown in Figure 1 and compared the mixing time between them. The model is based on the following assumptions:

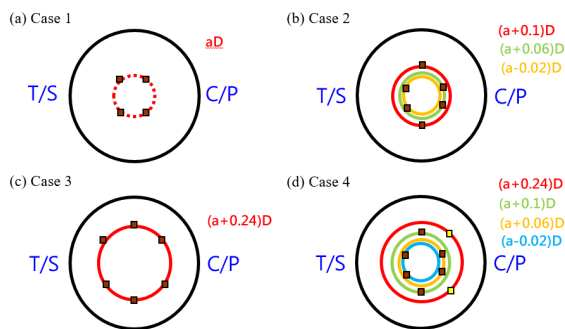


Fig.1. Bottom tuyere distribution. (a) 4-hole concentric, (b) 6-hole non-concentric, (c) 6-hole concentric, and (d) 8-hole non-concentric.

- (1) Since this study mainly investigated the effect of bottom blowing distribution, the interaction with the top blowing flow is ignored.
- (2) Liquid metal could flow along the gas-liquid interface, and the bottom blowing gas could rise to the surface and escape into the atmosphere.
- (3) The velocity of bubbles entering the bath was calculated according to the gas flow rate and tuyere diameter.
- (4) Since the bottom blowing distribution was symmetric, this study only simulated half of the bath.
- (5) The Eulerian-Eulerian model is adopted to simulate the gas and liquid flow behavior respectively.
- (6) The gas-liquid interaction is coupled by Stoke's flow theory.
- (7) The bubble can't penetrate the bottom and side wall.
- (8) The bath adopted no-slip condition.

A schematic diagram of representative grid division

is shown in Figure 2. The mesh is further refined to capture detailed flow behavior near the bottom blowing inlets. This study presents a transient simulation and the distribution of concentration at different times which indicates the mixing phenomenon is simulated. In addition, the shear stress contour of refractory lining is also simulated to evaluate the erosion characteristics. Finally, the simulation results are compared with the measured erosion rate and metallurgy data to find the optimal bottom tuyere distribution.

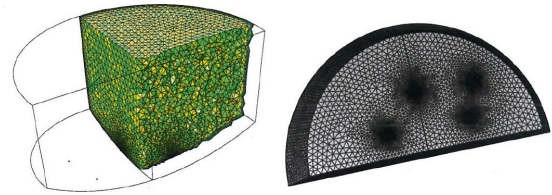


Fig.2. Schematic diagram of representative grid division.

3. RESULTS AND DISCUSSION

3.1 Mixing Characteristics of Molten Bath

Figure 3 presents the transient concentration distribution for four designs without consideration of the top blowing effect. The simulated results for Case 1 show that it has the slowest mixing rate, while Case 4 has the fastest. On the other hand, although both Case 2 and Case 3 use a 6-hole design, the difference in concentration distribution becomes increasingly apparent as the blowing progresses. A higher mixing rate is observed in Case 2, resulting in a relatively homogeneous concentration by the end of the simulation. This suggests that a non-concentric distribution facilitates better mixing compared to a concentric one. Additionally, with the inclusion of two extra bottom tuyeres on the charging side in Case 4, superior mixing is achieved and a complete mixing is found by the end of the simulation.

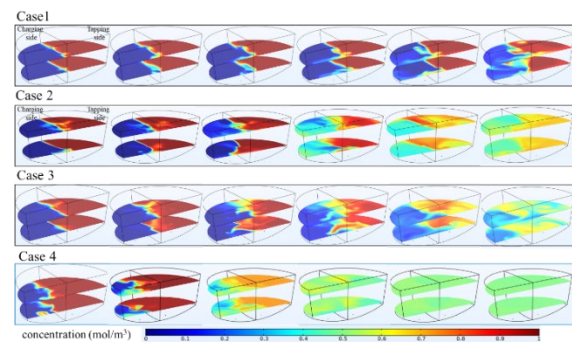


Fig.3. Distribution of concentration at 2, 4, 6, 8, 10, and 12 minutes for four cases.

3.2 Erosion Rate of Tuyere Bricks

The lining life of the bottom tuyere is a very important factor for basic oxygen furnace metallurgy. The erosion rate varies with different positions of tuyeres. Figure 4 shows the abnormal erosion rate of the tapping side for Case 3. Comparing Case 3 with the other cases, Case 3 attempts to widen the bottom tuyere distribution to reduce the dead zone, which is the region with the slower mixing rate. Tuyeres at the tapping side for Case 3 are much farther from the center than the other cases. They easily soak on the interface between slag and steel in the period of tapping. Slag and steel in this interface contain high oxygen potential, which easily oxidizes the graphite in the tuyere brick at high temperatures. Graphite plays a very important role in resisting slag corrosion and the thermal shock in MgO-C refractory brick due to low thermal expansion and poor wettability with slag⁽⁵⁾. Thermal shock means that the thermal stress varies with temperature and then bricks are easily peeled off. The above-mentioned explanation is the main cause of the abnormal erosion rate in Case 3. Due to the phenomenon of abnormal erosion rate at the tapping side, Case 4 attempts to shift the tuyere bricks on the tapping side toward the center, compared to Case 3. Figure 5 shows that the erosion rate of Case 4 is 11% lower compared to Case 3. In addition, Figure 6 shows that the extra two tuyeres at the charging side, tuyere #5 and #8, are much thicker than the others. The two newly added bottom tuyeres are more likely to survive until the converter goes to this generation shutdown.

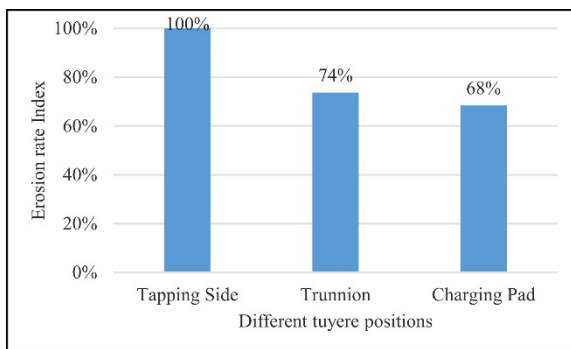


Fig.4. Comparison of erosion rate index of tuyere bricks at different positions for Case 3.

3.3 Shear Stress Contour of Refractory Lining

The distribution of bottom tuyeres not only affects the flow field of the molten bath but also creates areas of the shear stress concentration, leading to abrasion. A stress concentration phenomenon occurs in a localized region where the stress is significantly higher than in the surrounding area. Although the above-mentioned

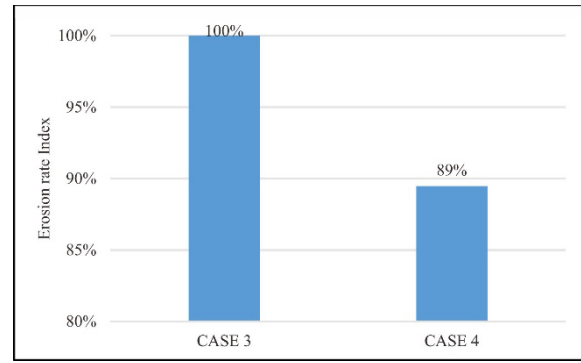


Fig.5. Comparison of erosion rate index between Case 3 and Case 4.

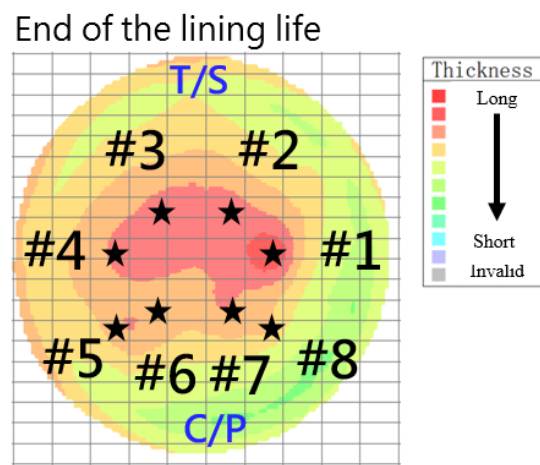


Fig.6. The thickness of the bottom contour for Case 4 at the end of lining life.

contents show the bottom stirring ability in Case 4 is the best among the four cases, the velocity and turbulent kinetic energy of the flow field are crucial factors in the abrasion caused by shear stress.

Figure 7 shows the distribution of shear stress around the tuyere bricks and the wall on the charging side, respectively. Since the comparatively stronger liquid circulation impacts the wall on the charging side in Case 4 than in Case 1, a larger stress concentration region is found in Case 4. As mentioned in the literature, the velocity and turbulent kinetic energy generated by the flow field increase with the height of the molten bath⁽⁶⁾. This phenomenon is particularly pronounced in the slag-line region, where gas, slag, and metal interact intensely leading to wall wear. However, field measurements show that there is no abnormal erosion is observed for high shear stress region as indicated in in Figure 8. Figure 7 shows the maximum shear stress was 0.12 Pa and much smaller than the theoretical value of MgO-C brick, which was usually about 10~30 MPa. It is the main reason why Case 4 can't find abnormal erosion in the shear stress concentration region.

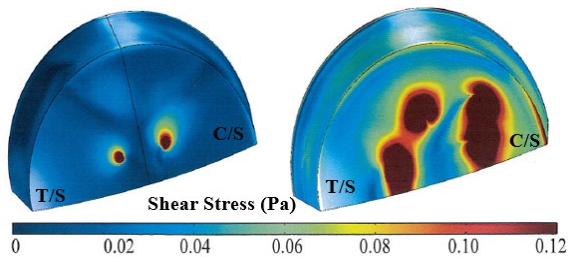


Fig.7. The shear stress distribution for Case 1 and Case 4.

3.4 Metallurgy Phenomenon

All cases adopt the same blowing parameters, which include the oxygen blowing intensity, the gap between the lance tip and bath, and the bottom blowing intensity. Table 1 presents the dephosphorization rate of both four cases are similar. After a full period of lining life, total iron in the slag (T.Fe) of Cases 2 and 4 is better among the four cases. T.Fe corresponds to the amount of Fe_xO_y (FeO and Fe_2O_3). Excess Fe_xO_y attacks the dicalcium silicate layer and then a phosphorus reversal reaction exists. In addition, much higher T.Fe means higher iron loss. Although the T.Fe of Case 2 is similar to that of Case 4, the initial tuyeres in Case 4 are more than in Case 3. There are likely more tuyeres toward the end of

lining life in Case 4. Figure 9 shows that T.Fe is related to the number of tuyeres. T.Fe theoretically increases near the end of the blow. Towards the end of the blow, the T.Fe depends on the blowing pattern and the carbon content of molten steel. T.Fe can be controlled by post-stirring to decrease iron loss, so Case 4 is more likely to control T.Fe toward the end of lining life. Table 2 shows T.Fe keeps a similar value although the tuyeres on the tapping side turn off due to erosion.

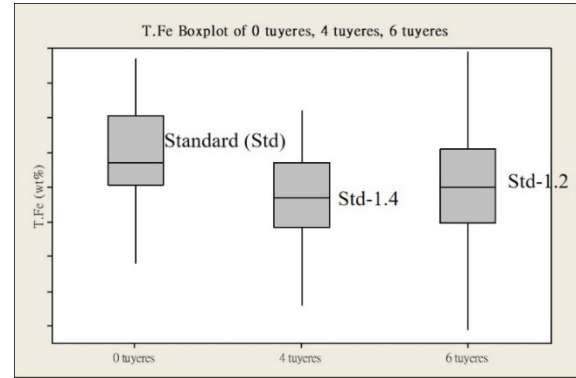


Fig.9. T.Fe variation with the number of tuyeres.

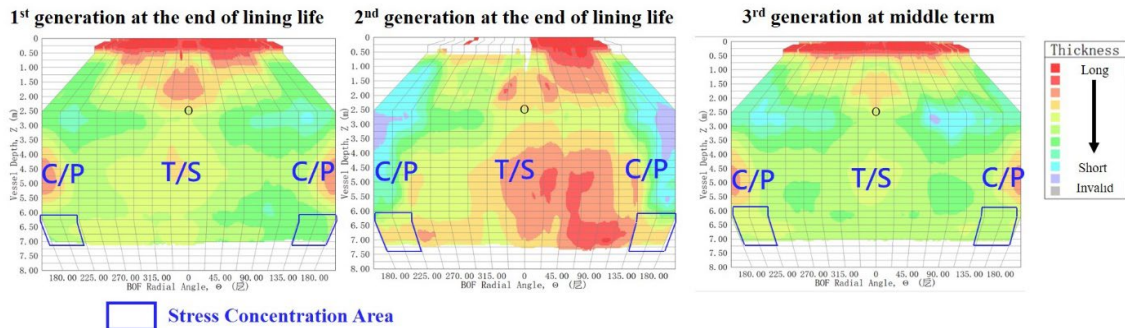


Fig.8. Shear stress concentration regions at the wall side for Case 4.

Table 1 The metallurgy data for four cases.

Metallurgy Data	Case 1	Compared to Case 1		
		Case 2	Case 3	Case 4
Dephosphorization rate (%)	Standard	-0.4	0.6	0.4
Basicity	Standard	-0.2	+0.1	+0.1
MgO _{slag} (wt%)	Standard	+0.6	+1.8	+2.8
T.Fe (wt%)	Standard	-1.9	-0.6	-2.0

Table 2 The metallurgy data for Case 4 with and without bottom blowing on the tapping side.

Metallurgy Data	Case 1	Blowing on the tapping side for Case 4	
		with blowing	without blowing
Dephosphorization rate (%)	Standard	-0.1	-0.5
Basicity	Standard	0.1	-0.1
MgO _{slag} (wt%)	Standard	2.6	2.6
T.Fe (wt%)	Standard	-2.6	-2.0

4. CONCLUSION

The bottom tuyere distribution plays a very important role in basic oxygen furnace metallurgy. The suitable distribution not only can shorten the complete mixing time of the molten bath but also avoid abnormal erosion of tuyere brick in particular positions. Case 4 integrates the advantages of all cases to develop a novel 8-hole non-concentric bottom blowing design. There were three advantages in Case 4.

- (1) Let the tuyere position near the tapping side move to the center compared with the other cases. It shortens the time the tuyere brick was soaked in high-temperature slag and steel, and then oxidation of graphite in tuyere brick can be inhibited.
- (2) By adding the extra two tuyeres at the charging side, the number of tuyeres in Case 4 is more than that of the other cases toward the end of lining life. Case 4 can effectively control T.Fe and decrease iron loss over the entire generation.
- (3) Bottom blowing design adopts non-concentric tuyere distribution. When the remaining lining thickness decreased, the contact surface of the brick decreased and binding strength among the bricks dramatically weakened. For concentric design, if one tuyere brick causes abnormal erosion, it will increase the risk that the other tuyere bricks fall due to the decrement of binding strength among bricks.

Case 4, the 8-hole bottom tuyere distribution, indeed avoids the abnormal erosion of tuyere bricks and improves BOF metallurgy. It reaches the goal of high efficiency, long-life top and bottom combined blowing in a 150-ton converter. Figure 10 presents Case 4 has the highest proportion of producing ultra-low phosphorus steel in the late period of lining life. It can increase the ability to produce high-value refined steel over the entire generation.

REFERENCES

1. Libin Yang, Jiaqing Zeng, Yong Deng, Xiaowei Xu, Liping Wu: "Highly efficient and long-life combined blowing technology of big converter". *Iron and Steel*, 2020, vol. 55(4), pp. 45-52.

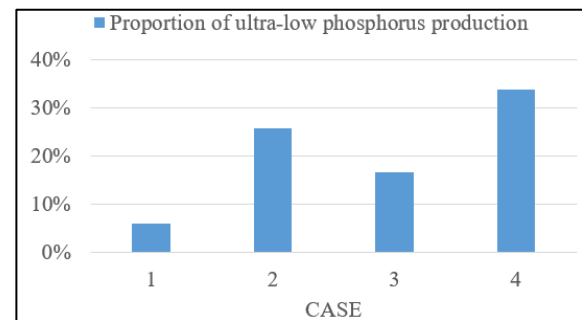


Fig.10. Proportion of producing ultra-low phosphorus products in the late period of lining life.

2. Dong Li, Jiaxue Hu: "Status of research and application of plug for combined blown converter in China and its trend of development". *China Metallurgy*, 2012, vol.22(2), pp. 7-9.
3. Zhoug Wang, Shuang Chen, Congcong Wu, Nan Chen, Jiwen Li, Qing Liu: "Effect of bottom stirring on bath mixing and transfer behavior during scrap melting in BOF steelmaking: A review". *High Temperature Materials and Processes*, 2024, vol. 43(1), pp. 20220322
4. Liangcai Zhong, Yingxiong Zhu, Xingfu Zeng, Zhaoyi Lai, Boyu Chen: "Technology of bath stirring in top and bottom combination blown converters and its application". *Steelmaking*, 2016, vol. 32(5), pp. 1-10.
5. Zhaoyang Liu, Jingkun Yu, Xin Yang, Endong Jin, and Lei Yuan: "Oxidation Resistance and Wetting Behavior of MgO-C Refractories_Effect of Carbon Content". *Materials*, 2018, vol. 11(6), pp. 883.
6. Jiankun Sun, Jiangshan Zhang, Rui Jiang, Xiaoming Feng, Qing Liu: (2023). "Effect of Bottom Tuyere Arrangement Based on Impact Cavity Morphology on Kinetic Behavior of Molten Bath in Converter". *Steel Research*, 2023, vol. 94, pp. 2200532.